https://doi.org/10.5194/egusphere-2026-5283
Preprint. Discussion started: 3 September 2026

Simulations of water transport over the Iceland–Scotland Ridge improved by local grid refinement around the Faroe Islands

Andrea M. U. Gierisch [1], Bogi Hansen [2], Karin Margretha. H. Larsen [2], and Steffen M. Olsen [1]

[1]National Center for Climate Research, Danish Meteorological Institute, Sankt Kjelds Plads 11, 2100 Copenhagen, Denmark
[2]Faroe Marine Research Institute, Nóatún 1, 100 Tórshavn, Faroe Islands

Correspondence: Andrea M. U. Gierisch (ang@dmi.dk)

Abstract. In the region between Iceland and Scotland, the warm water currents towards north and the cold water currents towards south are crossing a submarine ridge. Due to this complex bathymetry it is challenging for large scale ocean models to simulate the water flow realistically. High-resolution models perform better but are computationally more expensive. In this study, we investigate whether refining the model grid locally between Iceland and Scotland can improve the simulation of both the warm Atlantic water inflow and the cold deep overflow. The model grid is refined from 10 km to 3.3 km by using a two-way nest in a regional setup of the NEMO-TOP ocean model. A dye passive tracer is used to clarify the course of cold overflow water masses. Comparing the simulated water transports with in-situ observations around the Faroe Islands illustrates the benefit of the nest: 1) With the nest, more Atlantic water flows over the Iceland–Faroe Ridge and less through the Faroe–Shetland Channel, hence correcting the under-/overestimation seen in the coarse resolution model. 2) Overflow of deep water in the Faroe Bank Channel is increased by the nest to 2.14 Sv, which resembles well the observed value of 2.22 Sv. Additionally, the dye passive tracer simulation reveals that the nest enables the overflow water masses to decent to greater depths. These results indicate that the use of a local grid refinement by a two-way nest in a confined region is a promising and cost-efficient approach for improving the simulation of large scale water transports in the Atlantic.

1 Introduction

Around the Faroe Islands, warm and cold ocean currents pass over the Iceland–Faroe–Scotland Ridge as part of the large-scale Atlantic Meridional Overturning Circulation (AMOC). In the AMOC, cold and dense water masses flow southward in the deep ocean while warm Atlantic water from the South is transported towards the Arctic in the upper ocean. In the area around Iceland and the Faroe Islands, these water currents cross a submarine ridge spanning from Greenland to Scotland (Greenland–Scotland Ridge, GSR), which obstructs the water flow and hence is important for the water exchange between the Atlantic and the Nordic Seas. The main inflow of warm Atlantic water takes place between Iceland and Scotland (Østerhus et al., 2019; Rossby et al., 2018) and also a large part of the overflow is seen there (Olsen et al., 2008; Bringedal et al., 2018). Therefore, we focus this study on the area around the Faroe Islands. The major water transport routes are illustrated in Fig. 1: One branch of warm Atlantic water flows south around the Faroe Islands and then northward along the slope of the Faroe–Shetland Channel (FSC). Another branch of Atlantic water passes over the Iceland–Faroe Ridge (IFR), where the bathymetry is complex, leading

https://doi.org/10.5194/egusphere-2026-5283
Preprint. Discussion started: 3 September 2026

to variable flow with eddies and recirculations. Close to the Icelandic shelf, the Atlantic water crosses the ridge in a narrow strong jet, but most of the inflow is seen on the eastern side closer to the Faroes as a broad but slower flow (Hansen et al., 2023, Fig. 14). After crossing the IFR, the Atlantic water turns southeastward following the slope where it confines to the Faroe Current (e.g. Rossby et al., 2009; Hansen et al., 2010). that can be observed at the hydrographic section "Section N". Overflow of cold, dense water takes place mostly through the Faroe Bank Channel (FBC), which has the deepest sill, but smaller amounts of overflow also occur over the Wyville–Thomson Ridge and over the Iceland–Faroe Ridge (Hansen and Østerhus, 2000).

Simulating these water mass transports over the Greenland–Scotland Ridge is challenging for large-scale climate models, which cannot resolve the complex bathymetry nor the interaction with mesoscale eddies of some of the water flows (Wang et al. (2015); Jackson et al. (2023)). Even climate models with higher resolution than standard CMIP6 models often struggle to simulate realistic overflow (Roberts et al., 2020). For example, in simulations of Adcroft et al. (2019) with 1/2° and 1/4° resolution, overflow from the Nordic Seas is diluted too much and does not sink below 1000 m. This, however, can be problematic for realistic simulations of the lower limb of the AMOC (Zhang et al., 2011).

A key parameter for realistic simulations with global ocean models is the horizontal resolution as explained by Hewitt et al. (2017). Wang et al. (2015) found that AMOC simulations are sensitive to the grid specification near overflow channels. Interestingly, a high *horizontal* resolution is more important than a high *vertical* resolution for overflow simulations (Colombo et al. (2020); Riemenschneider and Legg (2007)), at least when using z-level vertical coordinates like many global ocean models do. The model resolution also has an influence on simulations of the future decline of the AMOC where higher-resolution models show a stronger AMOC decline (Hewitt et al., 2020).

Hence, many benefits can be expected from running global climate models in very high resolution, which is currently pursued by the Destination Earth digital twin for climate change adaptation (Doblas-Reyes et al., 2026). This approach is, however, computationally extremely demanding. To overcome this challenge, grid refinement methods have been developed, which allow for an increased resolution in key areas of the model domain while keeping other areas at a lower resolution. In this study, we deploy the two-way nesting approach implemented using the Adaptive Grid Refinement In Fortran (AGRIF) (Debreu et al., 2008). This approach has been applied already in previous modelling studies, for example Talandier et al. (2014) have refined the North Atlantic region by embedding a 1/8° two-way nest into a global 1/2° model, which resulted in a considerably stronger AMOC. Also Bezaud et al. (2026) have refined the North Atlantic region by applying a double two-way nest in a global 1° model to achieve a local resolution of 1/12°. Biastoch et al. (2018) tested an AGRIF nest for the Agulhas region around South Africa and found it to be computationally cheaper than an unstructured-mesh grid.

All these studies have implemented their high-resolution nests for rather large spatial areas like the whole northern North Atlantic. But are these large domains necessary or could some improvement for water transport simulations also be achieved by a more localized, cheaper nest? To answer this, we explore in this study a 2-way nesting approach where we refine the resolution of an ocean model only in the critical area between Iceland and Scotland, and we investigate whether this can improve the simulation of AMOC-related water transports around the Faroe Islands by evaluating the model simulations against observations.

https://doi.org/10.5194/egusphere-2026-5283
Preprint. Discussion started: 3 September 2026

We proceed like this: In Section 2, we first introduce the model setup and the experiment design, namely a nested simulation and a non-nested simulation as reference (Sect. 2.1). To analyse the pathway of overflow waters, we apply a dye passive tracer approach, which is explained in Sect. 2.2. To eventually evaluate the skill of the nested model simulation, observational data of sea surface height and water mass transports are used, which are described in Sect. 2.3. The results of the comparison between nested and non-nested simulations are presented in Sect. 3. In Section 4 follows a discussion of the effects of the nest on i) the inflow of warm Atlantic water over the Iceland–Faroe–Scotland Ridge, ii) the overflow of dense water in the Faroe Bank Channel and iii) the depth of sinking overflow waters. The Outlook (Sect. 4.5) describes the impact and possible future applications of the nesting approach, and the final conclusions are given in Sect. 5.

2 Modelling approach and Data

2.1 The NEMO-AGRIF model setup

Our model setup is based on the regional setup “NAA10km” of the ocean model NEMO (Madec et al., 2019) covering the North Atlantic and the Arctic region. It is presented in Hordoir et al. (2022) and has proven to run stably over several years even without assimilation or restoring. When upgrading their system from NEMO 3.6 to version 4.0.4 (r13658), we have adjusted only few model parameters. A summary of important parameters and settings is given in Table A1 in Appendix A. The simulations include tides, runoff and the inverse barometer effect. The model domain covers the Arctic and the North Atlantic (north of 40° N) with a resolution of 10 km. This setup is called ”Parent-Only”.

To study the effect of a local grid refinement around the Faroe Islands, we apply a two-way nest using AGRIF (Adaptive Grid Refinement In Fortran; Debreu et al., 2008). In this ”Nested” setup, the region between Iceland and the Shetland Islands is refined horizontally to about 3.3 km. Figure 1 shows the location of the nest and the model bathymetry. The bathymetry inside the nest is interpolated from the ORCA12 bathymetry; the vertical grid is the same as in the parent domain. AGRIF handles the boundary conditions of the nest automatically so that it receives information from the parent domain. In turn, the parent domain gets updated with the values calculated by the nest. With this, also areas outside of the nest are impacted by processes of the high-resolution domain. A bugfix for the routine that updates the parent model has been necessary to use in NEMO 4.0.4 when running the model with non-linear free surface. The applied code changes are available as Supplementary Material S1.

https://doi.org/10.5194/egusphere-2026-5283
Preprint. Discussion started: 3 September 2026

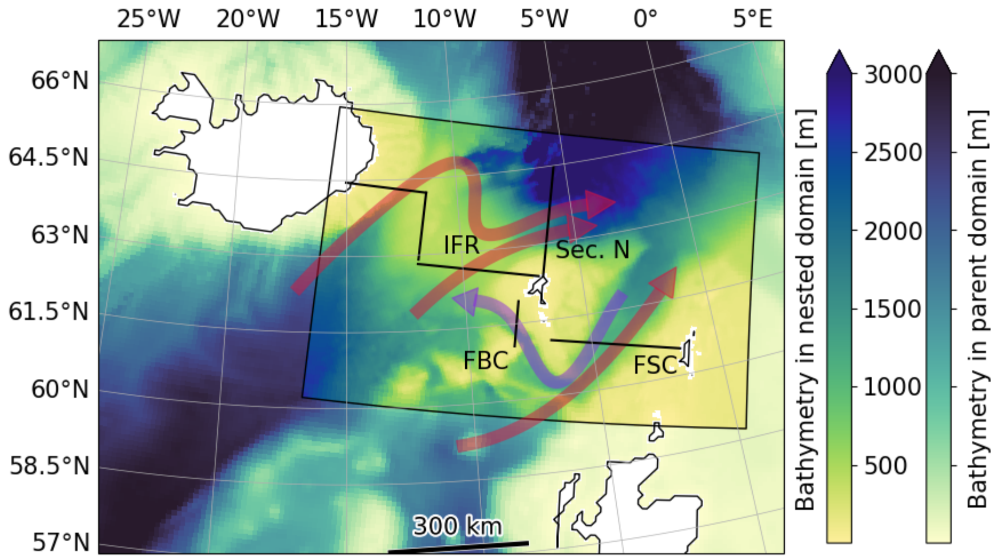

Figure 1. Bathymetry in the area of interest. The location of the nested model domain is indicated by a black box and a different colormap. Relevant warm and cold ocean currents are depicted as red and purple arrows, respectively. The locations of sections used in this study are shown as black lines: Faroe Bank Channel (FBC), Faroe–Shetland Channel (FSC), Section N (Sec. N), and Iceland–Faroe Ridge (IFR).

The Nested model is initialized in September 2007 with water temperatures and salinity from the ORAS5 reanalysis (Zuo et al., 2019). At the surface, the model is forced by atmospheric data from the ERA5 reanalysis (Hersbach et al., 2020) with 3-hourly values of wind components, short wave and long wave radiation, 2–m temperature, specific humidity, total precipitation, snow fall, and sea level pressure. At the lateral boundaries of the parent domain, monthly values of barotropic ocean currents, sea surface height, water temperature, salinity and ice conditions are prescribed from GLORYS (https://doi.org/10.48670/moi-00021). When the Nested model run reaches 1 March 2014 (i.e. after 6.5 years of spin-up), the Parent-Only simulation is branched off by disabling the nest. This Parent-Only simulation serves as a reference for investigating the effect of the nest. Both simulations run until the end of 2020, and model output is saved as monthly or daily averages for full field data and as hourly averages on the sections shown in Fig. 1 (FSC, FBC, Sec. N and IFR). The hourly output frequency was required to correctly calculate the transport of water of certain temperature and salinity in highly variable flow conditions. (See also Appendix B.)

2.2 Setup of the dye passive tracer simulations for overflow waters

After overflow water has crossed the Greenland–Scotland Ridge, it sinks to deeper levels while partly being mixed with surrounding waters. Therefore, it is difficult to assess its pathway based on temperature and salinity only. To overcome this, we use dye passive tracers simulated with the NEMO tracer module NEMO-TOP ("Tracers in Ocean Paradigm"; NEMO TOP Working Group (2018)). At the start of each tracer simulation, a tracer value of 100 % is assigned to all grid cells north of the Greenland–Scotland Ridge with water colder than 2 °C and salinity higher than 34.9 psu. During the course of the simulation,

https://doi.org/10.5194/egusphere-2026-5283
Preprint. Discussion started: 3 September 2026

tracers are transported by the water currents at every model time step. They can freely cross the boundary between the nested and the non-nested regions, like any other model quantity. The diffusion settings for tracers are the same as for temperature and salinity so that tracer values indicate the amount of original cold deep water in each grid cell. As this study focuses on the region between Iceland and Scotland, tracer values are set to zero in a "deletion zone" between Greenland and Iceland (Denmark Strait). With that, the total amount of Iceland–Scotland overflow can be calculated by spatially integrating all traced water volume south of the ridge. For long simulations there are two risks: Firstly, the tracer reservoir north of the ridge might get depleted and secondly, traced water might leave over the lateral boundaries of the parent domain. To avoid these, we reset the tracer fields to the initial values every year during the model restart in March. Resetting once a year is sufficient as will be demonstrated in Sect. 4.3. Tracer simulations are carried out for both the Nested and the Parent-Only setups and tracer fields are saved as daily averages.

2.3 Evaluation data

To evaluate the effect of the nest on model performance we compare the model output to observations. The simulated sea surface height, which is an indicator of the general circulation pattern, is evaluated against an altimetry product. The specific water mass transports around the Faroe Islands are assessed on three sections for which there exist robust, long-term observations, based on in situ and satellite data. The time series used are: a) transport of Atlantic water in the Faroe–Shetland Channel, b) transport of Atlantic water at Section N and c) transport of overflow water in the Faroe Bank Channel.

Sea surface height is evaluated against the altimeter product SEALEVEL_GLO_PHY_L4_MY_008_047 from the Copernicus Marine Service (https://doi.org/10.48670/moi-00148, accessed on 2024-10-03). For this, daily values of Absolute Dynamic Topography (ADT) from March 2014 until December 2020 are remapped from the original 0.125°-grid onto the NEMO model grid. Then, the spatial average is subtracted and the time average over the model period is calculated. The model output which shall be compared to these observations has been processed as follows: From the simulated daily sea surface height (zos) we remove the part caused by the inverse barometer effect (ssh_ib) because this effect is not included in the altimeter product. Similarly, as the tidal effect is also not included in the altimeter product, a 14–day running average is used for the model output to remove spring/neap tide effects. Subtracting the spatial mean and calculating the time average over the model period yields the product that is comparable to the observations and it is called "SSH-pattern" (sea surface height pattern) in Sect. 3.1.

The **inflow of Atlantic water in the FSC** is evaluated against a time series of observations based on altimetry data. The procedure for deriving Atlantic water transport from altimetry has been introduced by Berx et al. (2013), but as the altimeter product has been updated since, we have adopted their method to the new version, namely the global gridded sea level anomaly (SLA) field SEALEVEL_GLO_PHY_L4_MY_008_047 from the Copernicus Marine Service (https://doi.org/10.48670/moi-00148, accessed on 2024-10-03). The updated version takes into account the changes in the altimetry grid and processing.

The **inflow of Atlantic water at Section N** is evaluated against observed monthly averaged volume transport of Atlantic water (defined as water warmer than 4 °C and saltier than 35.0 psu; see details in Hansen et al. (2015)). Transport values are derived from in situ observations combined with satellite altimetry and are available from 1 January 1993. Details on the

https://doi.org/10.5194/egusphere-2026-5283
Preprint. Discussion started: 3 September 2026

calculation method can be found in Hansen et al. (2023) and the data is available at https://www.envofar.fo/index.php?page=climate.

The **overflow in the FBC** is evaluated against observed kinematic volume transport. Daily transport values are derived from in situ observations in the FBC since November 1995 except for annual servicing periods of 2–3 weeks duration. Kinematic overflow is determined from the velocity field, solely, but it is roughly equivalent to transport of water colder than 6 °C (Hansen and Østerhus, 2007; Larsen et al., 2024). The data is available at https://www.envofar.fo/index.php?page=climate.

3 Results

3.1 Sea surface height pattern around the Iceland–Faroe–Scotland Ridge

The impact of the model nest on the ocean simulation is first investigated based on the SSH-pattern described in Sect. 2.3. It reflects the geostrophic ocean currents and hence gives a good general overview of the model state. Figure 2 shows the SSH-pattern for the model simulations Parent-Only (Fig. 2(a)) and Nested (Fig. 2(b)) and compares it to the SSH-pattern observed by altimetry (Fig. 2(c)).

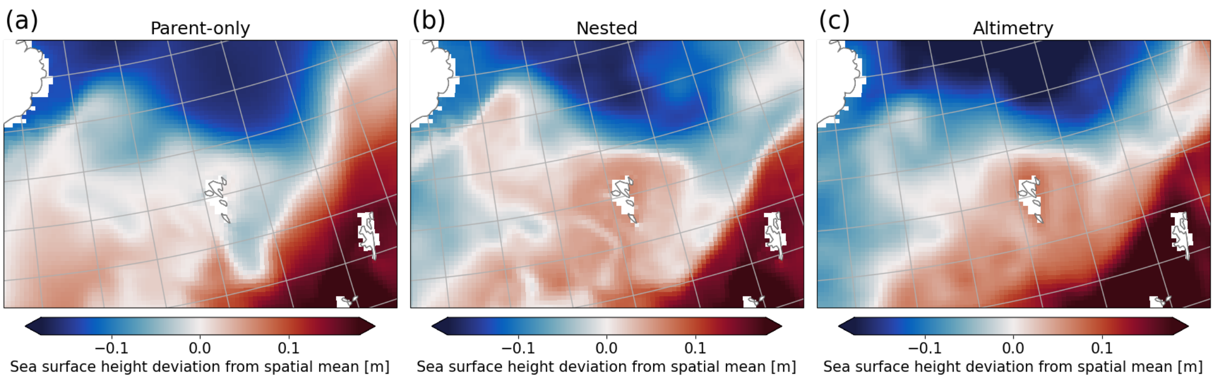

Figure 2. Time average SSH-pattern (deviation from spatial mean, excluding the inverse barometer effect) for the modelling period 2014–2020 for the Parent-Only simulation (a), the Nested simulation (b) and observations from altimetry (c).

In all products, the SSH-pattern shows higher values around the Scottish shelf compared to the regions north of the Iceland–Scotland Ridge. The altimeter product reveals that the sea level is relatively high around the Faroe Islands with a clear gradient both north and west of the Faroes. The elevated SSH levels around the Faroe Islands are also visible in the Nested simulation and the SSH gradient north of the Faroes looks similar to the observations. West of the Faroes, however, the Nested simulation does not reproduce the sharp gradient but it features high SSH-pattern values over the whole southern flank of the Iceland–Faroe Ridge and over the Rosengarten Bank (east of Iceland). The Parent-Only simulation is not able to reproduce the high levels of SSH around the Faroe Islands. Therefore, the SSH gradient is low both north and west of the Faroe Islands. East of Iceland however, the SSH-pattern of the Parent-Only simulation looks similar to the altimeter product. Also the Faroe–Shetland

Channel region is interesting for our study. Here, all three products differ considerably: The Parent-Only model simulates a strong SSH gradient that is not visible in the altimeter product. The Nested simulation features low SSH in the center of the Faroe–Shetland Channel with increasing sea level towards both the Faroe and the Shetland Islands.

3.2 Inflow of Atlantic water in the Faroe–Shetland Channel

To investigate the effect of the nest on the simulated northward flow of Atlantic water in the Faroe–Shetland Channel we utilize hourly model output of ocean currents, temperature and salinity on the FSC section visible in Fig. 1. From this, we calculate the monthly average volume transport of water warmer than 5 °C in the Nested and Parent-Only simulations, respectively. The threshold of 5 °C was chosen to match the criterion of the observational dataset (Sect. 2.3), which is used for the comparison.

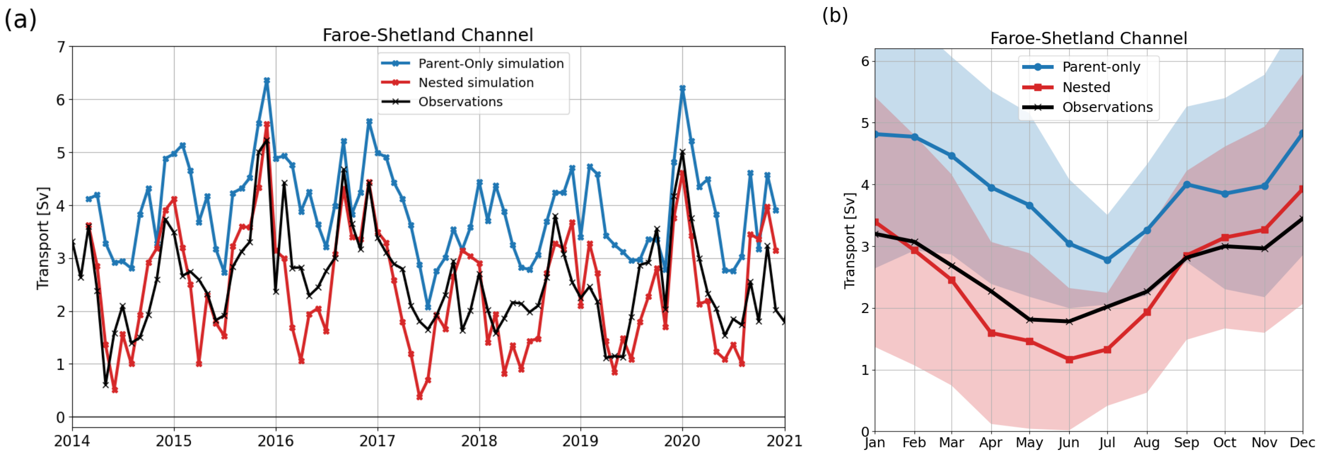

Figure 3. Inflow of water warmer than 5 °C in the FSC for the Parent-Only simulation (blue), the Nested simulation (red), and observations (black). (a) Time series of monthly averaged volume transport and (b) seasonality derived as monthly averages during the model period (Mar 2014 – Dec 2020). Shading indicates the range of ±1 standard deviation for daily values during all years.

Figure 3(a) shows time series of the northward warm water transport in the models and from observations. On average over the model period, a transport of 2.61 Sv is observed. The Parent-Only simulation overestimates this value considerably (3.93 Sv), while the Nested setup simulates a slightly too weak transport (2.44 Sv). Both modelled time series correlate well with the observed time series with Pearson correlation coefficients of 0.75 and 0.77 for the Parent-Only and the Nested simulations, respectively.

The climatology over the 7–year model period (Fig. 3(b)) shows that there is a clear seasonal signal in the warm water transport characterised by low inflow in late spring and high inflow in winter. Both models capture the seasonal cycle quite well in general. However, the minimum in spring is slightly delayed, mostly in the Parent-Only simulation, and too low in the Nested simulation. The daily variability indicated by the semi-transparent shading is considerably lower in summer time in the Parent-Only simulation. This feature is less pronounced in the Nested simulation, where there is high daily variability throughout the year. No daily observations of warm water transport are available for evaluation.

https://doi.org/10.5194/egusphere-2026-5283
Preprint. Discussion started: 3 September 2026

3.3 Inflow of Atlantic water at Section N

The other branch of Atlantic water flowing northwards is monitored at Section N, north of the Faroe Islands (Fig. 1). The hourly model output on this section is used to calculate the eastward transport of water warmer than 4 °C and saltier than 35.0 psu. These thresholds correspond to the definitions used in the observational data set. We refer to this warm and salty water as “Atlantic water“.

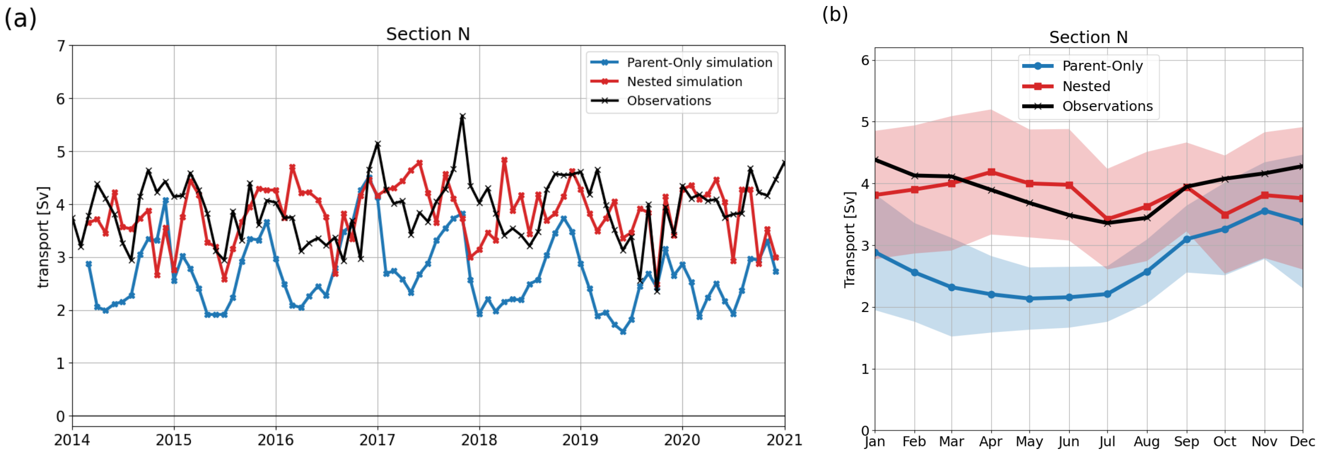

Figure 4. Inflow of water warmer than 4 °C and saltier than 35.0 psu at Section N for the Parent-Only simulation (blue), the Nested simulation (red), and observations (black). (a) Time series of monthly averaged volume transport and (b) seasonality derived as monthly averages during the model period (Mar 2014 – Dec 2020). Shading indicates the range of ±1 standard deviation for daily values during all years.

Monthly averages of the Atlantic water transport at Section N are shown in Fig. 4(a). The Parent-Only model (blue) simulates a transport of 2.69 Sv on average, which is much lower than the observed value of 3.91 Sv (black). The Nested simulation (red) performs much better in this respect and simulates an average transport of 3.83 Sv. In terms of correlation with the observed time series however, the Nested simulation performs worse than the Parent-Only simulation with Pearson correlation coefficients of 0.19 for the Nested and 0.44 for the Parent-Only simulations.

The reduced correlation is connected to a lack of seasonality as visible in the 7–year climatology in Fig. 4(b). The Nested model overestimates the Atlantic water transport in spring time and cannot reproduce the observed, small seasonal cycle. The Parent-Only model, on the contrary, overestimates the seasonal cycle because it simulates too little transport in spring. Regarding the daily variability, depicted as semi-transparent shadings, we see similar features as for the FSC: In summer time, the daily variability decreases in the Parent-Only simulation but not in the Nested simulation. There are unfortunately no observations to compare with.

https://doi.org/10.5194/egusphere-2026-5283
Preprint. Discussion started: 3 September 2026

3.4 Overflow of cold water in the Faroe Bank Channel

The effect of the nest on the simulation of overflow is analysed at the Faroe Bank Channel (FBC) section visible in Fig. 1. As evaluation data, we use observations of the kinematic FBC overflow, where "kinematic" best corresponds to waters colder than 6 °C (Hansen and Østerhus, 2007). With this threshold, we calculate the monthly averaged westward transport of overflow waters based on hourly model output.

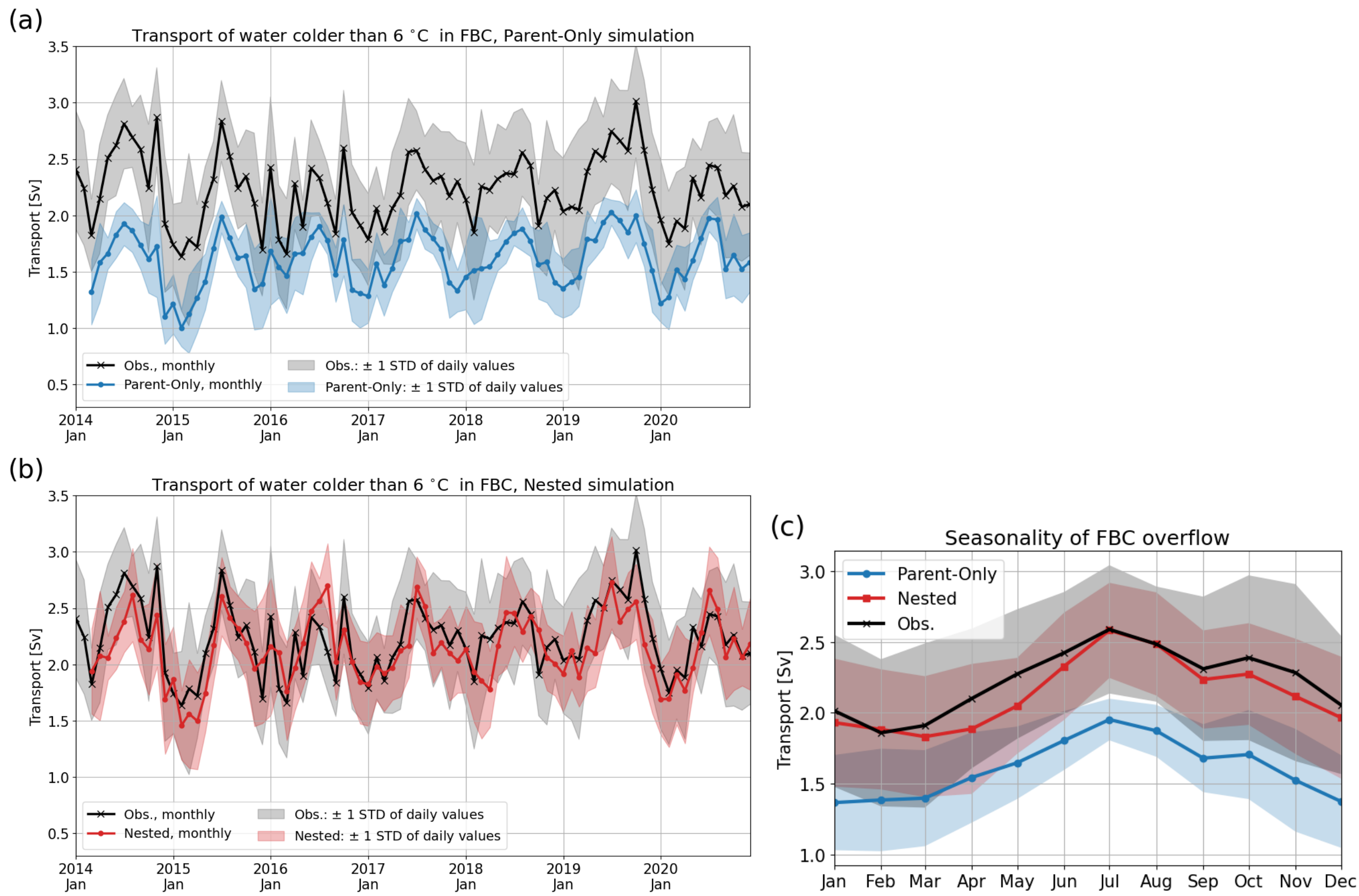

Figure 5. Overflow of water colder than 6 °C in the Faroe Bank Channel for the Parent-Only simulation (blue in (a) and (c)), the Nested simulation (red in (b) and (c)), and observations (black). (a)+(b): Monthly averages are shown as lines and shading indicates the range of ±1 standard deviation for daily values in each month. (c) Seasonality of FBC overflow during the model period (Mar 2014 – Dec 2020). Shading indicates the range of ±1 standard deviation for daily values during all years.

Time series of overflow are shown as solid lines in Fig. 5(a) for the Parent-Only simulation and in Fig. 5(b) for the Nested simulation, both compared to observations in black. The Parent-Only simulation underestimates the average overflow transport considerably with 1.61 Sv compared to the observed 2.22 Sv. However, the monthly variability is simulated very well as indicated by the Pearson correlation coefficient of 0.83. The Nested simulation performs much better with regard to the average

https://doi.org/10.5194/egusphere-2026-5283
Preprint. Discussion started: 3 September 2026

transport (2.14 Sv) but the Pearson correlation coefficient is a bit reduced (0.74). This could be connected to the underestimation of overflow in spring time as seen in the 7–year climatology in Fig. 5(c). The observed intensification of overflow during spring is delayed in the Nested simulation. However, maximum and minimum values in July and February, respectively, are simulated very well.

The daily variability of overflow is indicated by the semi-transparent shadings. Similarly to the inflow at FSC and Section N, the variability in the Nested simulation is generally higher than in the Parent-Only and this effect is most pronounced in summertime, where the Parent-Only model simulates a much too low variability compared to the observations. The Nested simulation is more realistic in this respect. It generally only slightly underestimates the observed variability of overflow.

3.5 Tracing the course of overflow waters downstream

Using dye passive tracers we can investigate the fate of the overflow waters after they have crossed the Iceland–Scotland Ridge and whether the nest affects this. Tracers are added to both the Nested and the Parent-Only setup, initially with values of 100 % for all water colder than 2 °C and saltier than 34.9 psu north of the Greenland–Scotland Ridge, called Overflow Water hereafter. During the model simulation, the tracer concentration at each grid cell indicates how much of the water volume consists of Overflow Water. The tracer concentration at bottom level after 12 months of simulation is shown in Fig. 6(a) for the Parent-Only setup and in Fig. 6(b) for the Nested setup. As a new tracer simulation is started every year, Fig. 6 presents the average state of these five yearly simulations.

https://doi.org/10.5194/egusphere-2026-5283
Preprint. Discussion started: 3 September 2026

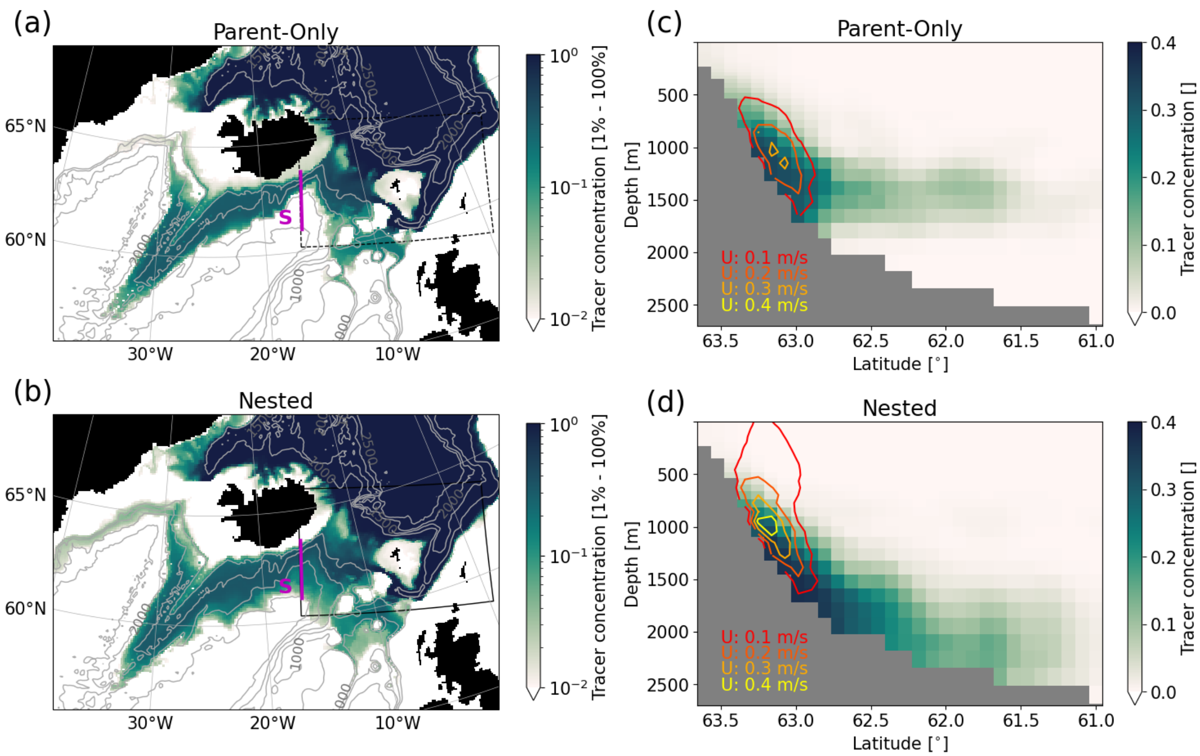

Figure 6. Tracer concentrations after 12 months of simulation at bottom level (left) and at section S (right), averaged over the five yearly simulations for Parent-Only (top) and Nested (bottom). (a)+(b): Grey contour lines depict bathymetry with 500 m intervals; the nested area is highlighted by a black box; the location of Section S is shown in magenta. (c)+(d): Contour lines depict the westward component of the current averaged over years 2015–2020 in 0.1 m/s intervals. Note the different color scales between map and section plots.

After 12 months, the amount of traced Overflow Water at bottom level is 100 % in the area north of the Greenland–Scotland Ridge, where tracers have been initialized. Tracer concentrations are also very high in the Faroe–Shetland Channel and in the Faroe Bank Channel, where the main overflow occurs. Overflow Water is also found over the Iceland–Faroe Ridge and south of the Wyville–Thomson Ridge, indicating that these are further overflow regions. Deducing from the high bottom tracer concentrations, the Overflow Water continues its way northwestwards along the southern slope of the IFR, turning westwards along the Suðurland slope south of Iceland and then following the Reykjanes Ridge. Along this pathway, the flow of tracers mostly follows the isobaths, however, differences between Nested and Parent-Only simulations emerge. With the nest (Fig. 6(b)), the traced Overflow Waters reach to deeper bottom levels in the Iceland Basin, while in the Parent-Only simulation (Fig. 6(a)) tracers are only found in areas higher up on the slope. Also further downstream, outside of the nested area, tracers reach deeper levels if the nest is applied.

The fact that the Overflow Water sinks deeper with the nest is also evident at Section S on the Suðurland slope: Fig. 6(c) and Fig. 6(d) show cross sections of tracer concentration and westward current speed for Parent-Only and Nested simulations, respectively. While the Overflow Water in the Parent-Only simulation is found mostly on the slope between 1000 m and 1500 m

https://doi.org/10.5194/egusphere-2026-5283
Preprint. Discussion started: 3 September 2026

depth and partly floating south off the slope at around 1500 m, the Nested model simulates traced waters all the way down the slope to below 2000 m depth. Additionally, with the Nested setup, there are higher tracer concentrations on the slope. The core of the westward current is located in a somewhat similar depth in both model setups but the speed is slightly higher with the nest.

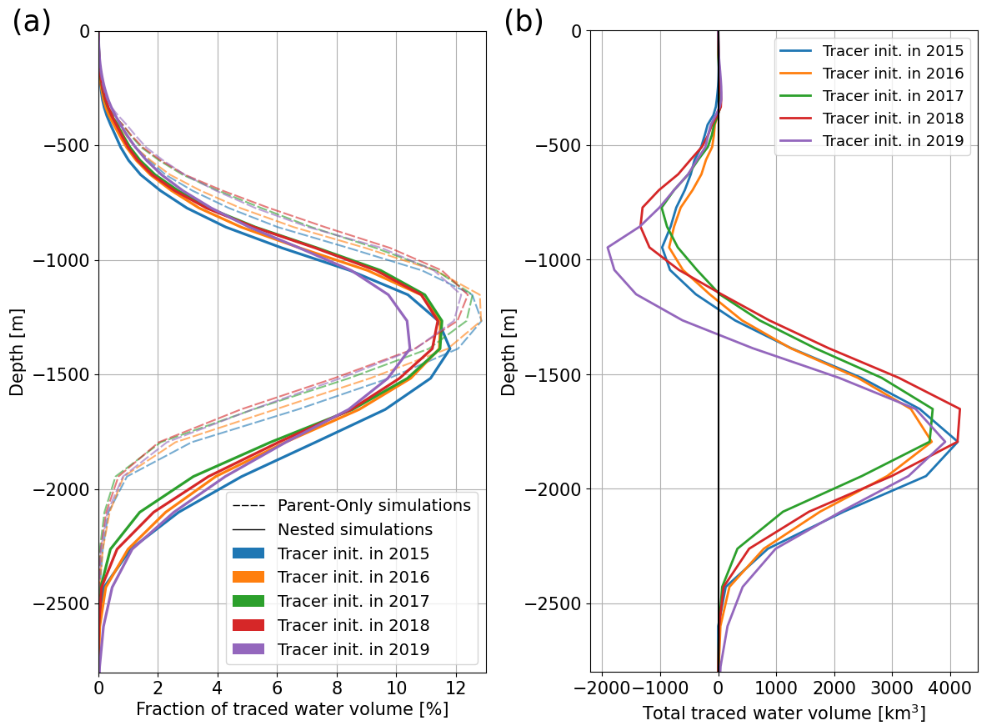

Figure 7. Depths of traced Overflow Water south of the Greenland–Scotland Ridge after 18 months of simulation, visualized by (a) the fraction of traced water volume at each depth level, with dashed lines representing the five Parent-Only simulations and solid lines representing the five Nested simulations, and (b) the absolute difference between Nested and Parent-Only simulations in total traced water volume at each depth level. The colors distinguish the five yearly simulations with tracers initialized between 2015 and 2019.

The general effect of the nest on the depth of Overflow Waters downstream of the ridge is investigated by average tracer profiles. For this, we spatially integrate the traced water volume of all grid cells south of the GSR separately for each depth level. Figure 7(a) shows which fraction of the Overflow Water is found at which depth. The model state after 18 months of simulation is depicted as dashed lines for the five different Parent-Only tracer simulations. The highest fraction of Overflow Water is found at around 1200 m depth and very little tracers reach below 2000 m in the Parent-Only simulations. With the nest however – as depicted by solid lines – the peak of the Overflow Water fraction is shifted down to 1350 m depth, and more than 2 % of the Overflow Water reaches below 2000 m by month 18.

Figure 7(b) presents the same data as Fig. 7(a) but showing absolute differences between Nested and Parent-Only simulations. The fact that the difference of total traced water volume is negative at depth levels above 1100 m clarifies that the

https://doi.org/10.5194/egusphere-2026-5283
Preprint. Discussion started: 3 September 2026

Overflow Water is indeed sinking deeper with the nest. Otherwise, the deeper peak in Fig. 7(a) could also have been caused simply by an increased amount of overflow in the Nested simulation.

4 Discussion

4.1 Inflow of Atlantic water over the Iceland–Faroe–Scotland Ridge

There are two main pathways of Atlantic water inflow over the Iceland–Scotland ridge: On the eastern side of the Faroe Islands, there is a confined inflow branch along the slope in the Faroe–Shetland Channel (FSC) while to the west of the Faroe Islands, the Atlantic water crosses the IFR in a more unsteady manner with recirculations and formation of eddies. The IFR inflow branch can best be monitored at Section N, where the flow narrows along the Faroese slope. The analyses in Sect. 3.2 and 3.3 show that the nest improves the simulated average Atlantic water inflow both in the FSC and at Section N: The overestimated inflow in FSC is reduced and the underestimated inflow at Section N is increased. However, the monthly correlation to the observed inflow time series does not improve, especially at Section N. The reason could be that the system is chaotic, especially over the IFR, and because the model is not assimilated or otherwise constrained towards observations, it produces a different realization of the chaotic system. Also, the inflow strength varies more from day to day if the nest is used (Fig. 3(b) and Fig. 4(b)), indicating that the Nested simulation can resolve more intermittent features. Due to the short simulation period of only 6 years, no conclusions are possible on the interannual variability, but the average flow pattern is robust. A good match between model and observations does not only indicate that the model simulations are realistic, but in turn it also confirms that the observation approach is adequate. It is not trivial to observe the Atlantic water transport as this involves a combination of in situ and remote sensing measurements as described in Hansen et al. (2023). Therefore, it adds confidence that our model can reasonably reproduce the observations.

4.1.1 Large-scale inflow pattern from altimetry

How the time series of Atlantic water inflow relate to the large scale flow around the Faroe Islands can be discussed using the average sea surface height pattern (Fig. 2). The gradient of the SSH-pattern reflects the geostrophic flow and it resembles well the features seen earlier for Atlantic water transport: **I)** North of the Faroe Islands along Section N, a sharp SSH gradient is visible both in the Nested simulation and in the observations whereas the gradient in the Parent-Only simulation is weak. This agrees well with the increased Atlantic water transport in the Nested simulation at Section N (Fig. 4). The nest is able to correct the flow pattern north of the Faroe Islands. **II)** In the central part of the Faroe–Shetland Channel, both the Parent-Only and the Nested simulation show a relatively too low sea level compared to the altimeter observations. In accordance with the too steep SSH gradient at the Shetland shelf slope, the Parent-Only model simulates too much inflow of Atlantic water in the FSC (Fig. 3). Even though also the Nested simulation creates a too steep SSH gradient over the Shetland shelf slope, the simulated Atlantic water inflow is lower with the nest. This can be explained by a stronger retroflection of the Faroe Current around the northeastern tip of the Faroe Plateau into the FSC as indicated by the pronounced SSH gradient over the Faroe Plateau

https://doi.org/10.5194/egusphere-2026-5283
Preprint. Discussion started: 3 September 2026

slope. This retroflection seems, however, to be overestimated in the Nested simulation: in the altimetry product, only a weak SSH gradient is visible across the Faroe Plateau slope east of the Faroes. **III)** Over the Iceland–Faroe Ridge, the SSH-pattern is complex with generally low sea level close to Iceland and higher sea level close to the Faroes. A region of high sea level usually present over the Rosengarten Bank, indicating some recirculation. The Parent-Only simulation is not able to reproduce the observed elevated SSH-pattern around the Faroe Islands, which corresponds to an underestimation of the total inflow over the IFR and especially over its eastern part. The Nested model simulates the relatively high SSH on the Faroe Plateau correctly; however, the gradient in the eastern part is anyway too low because the sea level over the Rosengarten Bank is overestimated. This means that we expect more total inflow over the IFR when using the nest, but with too much flow close to Iceland over the Western Valley and too little flow over the eastern part of the IFR. The latter should be the main inflow branch according to Rossby et al. (2018) and Hansen et al. (2023).

4.1.2 Inflow over the Iceland–Faroe Ridge and at Section N

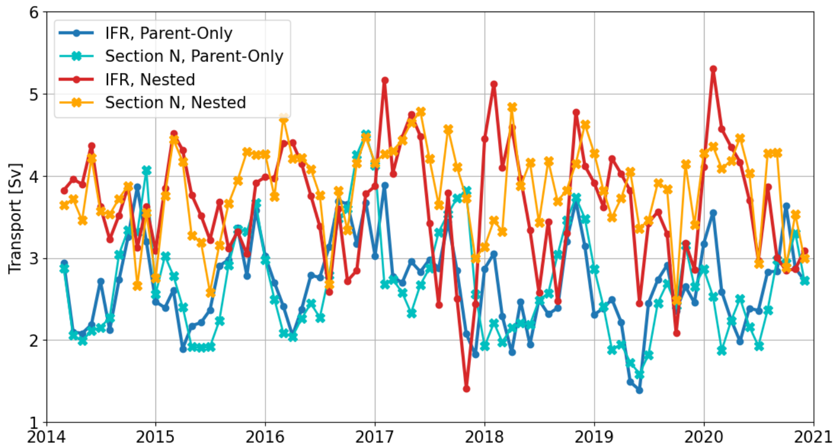

Figure 8. Simulated transport of water warmer than 4 °C and saltier than 35.0 psu over the IFR and at Section N by the Parent-Only model (blueish colors) and the Nested model (reddish colors).

The inflow of Atlantic water over the IFR is complex and difficult to observe directly, but after having crossed the IFR, the inflow confines to the Faroe Current and therefore the IFR inflow is usually monitored at Section N. For Section N, we have shown in Fig. 4 that the nest helps to increase the simulated Atlantic water inflow so that the average amount of inflow matches well with observations. Our SSH analyses suggest that also the total inflow over the IFR improves with the nest. To check this, we calculate the Atlantic water inflow over the IFR-section (location depicted in Fig. 1) and compare it to the simulated inflow at Section N. Figure 8 shows that the flow through Section N indeed resembles well the inflow over the IFR-section for both the Nested and the Parent-Only simulation. The mean transport over the IFR during the simulation period amounts to 2.70 Sv for the Parent-Only simulation and to 3.64 Sv for the Nested simulation. These values are quite close to the mean transport at Section N (2.69 Sv for Parent-Only and 3.83 Sv for Nested), hence the simulated inflow over the IFR is consistent with the inflow monitored at Section N. This means that the nest not only improves the simulation of Atlantic water inflow at Section N but also over the IFR. Hence, this improvement likely originates somewhere in the IFR region. A possible explanation could be that the higher spatial resolution allows the nest to resolve more eddying features, which are likely important for the inflow. As Eriksdóttir et al. (2026) explains, the Atlantic water flow before (=south of) the ridge is almost barotropic but in order for it to cross the isobaths of the IFR it needs to become more baroclinic. This is achieved by mixing on the flank of the IFR. Therefore, the model needs to be capable of resolving the many eddies that exist on and around the IFR (Beaird et al. (2016); de Marez et al. (2025)). The high-resolution Nested simulation indeed exhibits more SSH variability on the southern flank of the IFR: Figure 9 reveals that for the IFR flank, above the 1000 m isobath, the daily variability of SSH is increased. This indicates that the system is more dynamic than in the Parent-Only setup, which cannot resolve most of the small-scale eddying features. This, in turn, could explain why the coarse model underestimates the flow over the IFR.

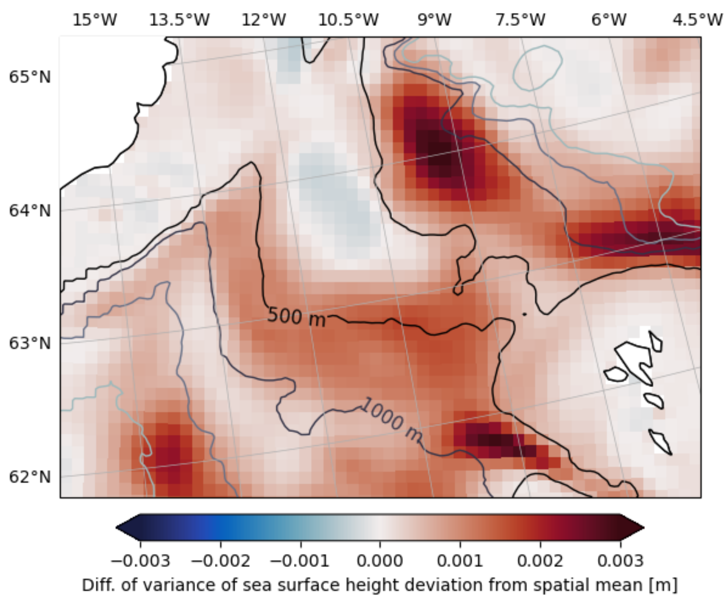

Figure 9. Effect of the nest on the simulated daily SSH variability (Nested minus Parent-Only). Red colors indicate that the Nested simulation features a higher time variance of the SSH deviation from spatial mean (as introduced in Sect. 2.3) compared to the Parent-Only simulation. Contour lines depict the bathymetry in 500 m intervals.

Why the nest corrects the overestimation of Atlantic water inflow via the FSC, can be speculated with a similar reasoning: The eddy features in the more dynamic system of the nest could disturb and thus reduce the main flow in the FSC compared to the Parent-Only simulation. Indeed, a correlation of a greater eddy activity in the FSC and a weaker Shetland Slope Current has been found already by Childers (2014).

https://doi.org/10.5194/egusphere-2026-5283
Preprint. Discussion started: 3 September 2026

4.2 Impact of increased resolution on the overflow in the Faroe Bank Channel

The high-resolution nest has a positive impact on the simulation of FBC overflow, both regarding the mean transport and the daily variability. As seen in Fig. 5, the Parent-Only model simulates too little overflow and with too little daily variability. The nest, again, seems to be better capable of simulating intermittent features and it represents a more dynamical system. Besides this effect, the higher horizontal resolution can improve the overflow simulation also due to other reasons:

Firstly, a higher resolution allows for a better representation of the bathymetry in the model grid. This is important in regions with steep bathymetry and narrow channels like the Faroe Bank Channel. If the width or depth of channels is inaccurately represented in coarse resolutions models, the simulated flow through the channel can be deteriorated. This is the case for example in climate models examined by Wang et al. (2015), where excessive channel width and depth lead to a too strong overflow in the Iceland–Scotland region; or a too narrow channel can block the overflow completely. However, also coarse resolution models can be able to simulate the overflow well but they might require a manually adapted/unrealistic bathymetry to do so as explained by Olsen et al. (2008).

A second reason for improved overflow simulations in high-resolution models can be the better representation of the flow structure itself. More grid cells can help to keep the flow plume confined as Riemenschneider and Legg (2007) has examined: Comparing models with resolutions between 50 km and 2 km, they show that large grid cells increase the entrainment, which influences how the dense water sinks down in the channel. In coarse models, the overflow plume becomes too thick and diluted due to enhanced vertical mixing. For this, Riemenschneider and Legg (2007) note that ”the numerical mixing in the model is found to be most sensitive to changes in the horizontal resolution, and to a lesser extent on vertical resolution“. This is an interesting effect, which has also been stated by Colombo et al. (2020), namely that an increased vertical resolution takes only effect if the horizontal resolution is sufficient (at least higher than 5 km). This supports our approach, where we increase the horizontal resolution from about 10 km in the parent domain to 3.3 km in the nest, while keeping the vertical resolution constant. Our result that the nest is beneficial for the simulation of FBC overflow seems reasonable.

Arguably, the vertical coordinate system of our model is not optimal for the simulation of overflows. Models with z-level coordinate systems often feature too much numerical vertical mixing. Better suited for cases like overflows, where isopycnals follow a slope, are for example isopycnal coordinate systems (Wang et al., 2015) or types of terrain-following coordinate systems (Bruciaferri et al., 2024). However, Hewitt et al. (2020) reports that the horizontal resolution is important for overflows regardless of the vertical coordinate system. So, a higher horizontal resolution is beneficial in all vertical coordinate systems, also in z-level systems. This underlines the value of our study, especially as many climate models also use z-level coordinate systems in their ocean models.

4.3 Using passive tracers to study overflow

For analyzing the fate of the overflow waters after crossing the ridge we use dye passive tracers as explained in Sect. 2.2. If a simulation is carried on for too long after tracers have been initialized north of the GSR, two problems might arise: a) The tracer reservoir in the North might become depleted and/or b) traced water can leave the model domain over the lateral model

https://doi.org/10.5194/egusphere-2026-5283
Preprint. Discussion started: 3 September 2026

boundaries. This would for example affect overflow estimates which are based on the increase over time of traced water south of the ridge. In both cases a) and b), the total overflow would be underestimated in the long run. To avoid this, we re-initialize the tracer field every year. Whether this re-initialization frequency is sufficient can be assessed by running simulations for more than one year and investigating whether the overflow strength drops. The overflow strength can be derived by integrating the traced water volume south of the GSR. The change in time of this total traced water volume corresponds to the overflow over the Iceland–Scotland Ridge (because tracers between Greenland and Iceland get removed). Time series of the tracer derived overflow strength are shown in Fig. 10.

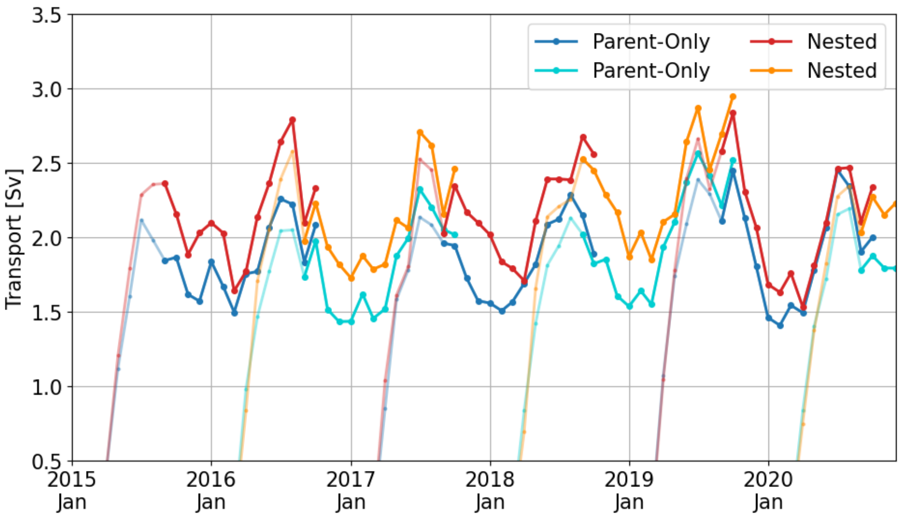

Figure 10. Monthly transport of Overflow Water over the Iceland–Scotland Ridge derived from tracer simulations for the Parent-Only setup (blue and turquoise lines) and for the Nested setup (red and orange lines). Alternating colors blue/turquoise and red/orange are used in the time series to distinguish the annually re-initialized tracer simulations. Semi-transparent lines indicate spin-up periods.

During the first ≈ 6 months after each re-initialization, the overflow strength increases gradually as the tracer flow to and over the ridge is building up. Hence, at least these months should be disregarded as spin-up. The tracer simulations are run annually for 20 months, hence they overlap for 8 months. Comparing "new" and "old" simulations reveals that the overflow strength does not decrease towards the end of the simulation period. Additionally, we have visually inspected the tracer fields after 20 month of simulation and found no signs of traced water leaving the parent model domain. Hence, a re-initialization frequency of one year is sufficient.

The overflow strength based on the tracer approach (Fig. 10) seems reasonable juxtaposing it with the overflow diagnosed at the FBC section (Fig. 5). The average flow and the monthly variability are similar and the nest increases the simulated overflow in both cases. The two values are, however, not directly comparable because they represent different physical quantities: The tracer approach includes all overflow over the Iceland–Scotland Ridge while Fig. 5 specifically focuses on FBC overflow. Also, the section-based overflow takes into account all water colder than 6 °C in the FBC while traced Overflow Water is water that has been colder than 2 °C at some point in time north of the ridge. Therefore, the overflow values are hard to compare, also with observations, but the tracer approach confirms that there is more overflow with the nest. The advantage of using tracers to determine the overflow lies in the fact that model output does not need to be saved with high time resolution. Monthly snapshots would be sufficient to calculate monthly average overflow from tracers, while the overflow calculation at the FBC section is sensitive to the frequency of the model output. This is due to the temperature-based masking of overflow water as explained in Appendix B. Moreover, the use of tracers to detect overflow water seems to be the more direct approach as it is independent of entrainment processes. Hence, it should be used complementarily to section-based investigations.

4.4 Depth of Overflow Waters

Utilizing the dye passive tracers we can investigate the pathway of the Overflow Water and especially the depth it reaches when descending downstream of the ridge. The average depth profiles of tracers (Fig. 7) clearly indicate that the Overflow Water sinks deeper when using the nest - on average by almost 150 m after 18 months simulation. The little variation of the profiles from year to year indicates a robust, recurring signal. The effect of the nest on the tracer depth is not restricted to the nested domain only, but tracers are found in deeper levels also after the Overflow Water has left the high-resolution area, as visible in Fig. 6(a,b). It highlights the benefit of using a local nest compared to a full high-resolution model, which would be computationally more expensive. This is supported by a recent study by Bezaud et al. (2026) who also see deeper penetration of overflow waters and a slight improvement on the simulated AMOC when using a nest in the North Atlantic.

A reason for the positive effect of the nest can be found in its reduced numerical diffusion and hence its ability to keep the overflow plume more confined and dense. This becomes evident in the bottom temperature field downstream of the Faroe Bank Channel sill, shown in Fig. 11. The bottom water after the sill, west of 8.5° W, is warmer in the Parent-Only simulation (Fig. 11(a)) than in the Nested simulation (Fig. 11(b)). Further downstream, the bottom water in the Nested simulation is able to sink down crossing the 1000–m isobath south of the "bump" B. This agrees well with observations (Beaird et al., 2013) but it is not reproduced by the Parent-Only model. Overall, the observed bottom temperature field presented by Beaird et al. (2013) in their Fig. 6(bottom) (based on sea glider observations) agrees quite well with our Nested simulation. With the nest, the overflow can follow the sloping bathymetry and stays confined as a cold and dense water mass at the bottom.

https://doi.org/10.5194/egusphere-2026-5283
Preprint. Discussion started: 3 September 2026

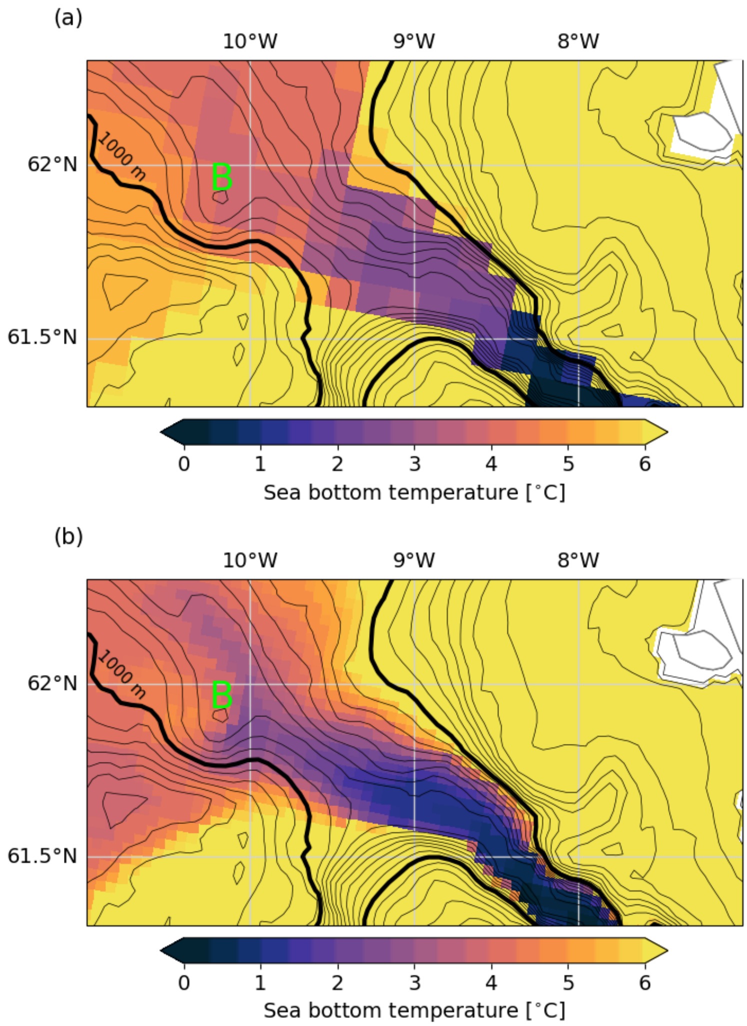

Figure 11. Potential temperature at sea bottom downstream of the Faroe Bank Channel sill in the Parent-Only simulation (a) and the Nested simulation (b). The bathymetry is depicted as contourlines every 50 m, with bold lines highlighting the 500–m and the 1000–m isobaths. The underwater bump is marked by "B".

Due to its high density and the high-resolution grid, the Overflow Water is able to continue its descent and it eventually reaches down below 1500 m on the Suðurland slope south of Iceland (Fig. 6(d)) and in the Iceland Basin (Fig. 6(b)). This is in good agreement with the modelling study by Guo et al. (2014), who apply the MITgcm model with very high horizontal and vertical resolution (2 km; 25 m). Their model also simulates deeply sinking overflow waters south of Iceland. Contrary, the models used by Adcroft et al. (2019) with horizontal resolutions of only 0.5° and 0.25° cannot reproduce this, and dense overflow waters do not penetrate below 1000 m depth. This highlights the importance of high spatial resolution for simulating descending overflows.

https://doi.org/10.5194/egusphere-2026-5283
Preprint. Discussion started: 3 September 2026

On Section S south of Iceland (Fig. 6(c,d)) it is visible that the nest not only promotes descending of traced water masses but that it also enables a higher speed of the slope current. Whereas the average current speed barely reaches 0.3 m s^{-1} in the Parent-Only simulation, there is a flow of 0.4 m s^{-1} with the nest. The effect that overflow speed can be reduced in coarse resolution models has also been reported by Riemenschneider and Legg (2007). Low resolution favours dilution and a more sluggish and slow flow. Compared to the recent high-resolution model of de Marez et al. (2024) (2 km; 80 topography-following levels), the result of our Nested simulation is promising: At Section S, the core of the flow in Fig. 1(c) of de Marez et al. (2024) reaches more than 0.35 m s^{-1} just below 1000 m depth. This is only slightly deeper and slower than the flow in our Nested model (Fig. 6(d)). However, a model by Xu et al. (2010) with hybrid vertical coordinates and 5 km horizontal resolution simulates a slower (0.25 m s^{-1}) but deeper (1700 m) flow. The few available observations from 1990 could also hint towards a deep flow, between 1300 m and 2100 m depth (Saunders, 1996), or at least with a core depth of 1300 m (Saunders, 2001). Even if not all of these reference data agree well with our model, we can conclude that the nest is nevertheless beneficial for the simulation of descending overflows.

4.5 Outlook

The Nested model generally shows a good performance compared to observations, but still with some limitations. Further improvements could potentially be achieved by an even higher spatial resolution as discussed in Sect. 4.2 and accordingly a finer resolved bathymetry in the nest. Overflow simulations would likely also benefit from more vertical levels or isopycnal/terrain-following coordinates and a better parameterization of the bottom boundary layer like presented in Hordoir et al. (2026). However, even in its current setup the Nested model exhibits considerable benefits over the Parent-Only simulation, which can have far-reaching implications:

An improved simulation of the inflow of Atlantic water over the ridge can have an impact on the heat transports. As shown in Fig. 2, the SSH-pattern southwest of the ridge and hence the inflow pathway are more realistic with the nest. This is supported by the transport time series showing that less Atlantic water flows via the FSC (Fig. 3) and more over the Iceland–Faroe Ridge (Fig. 8). The different ambient conditions in these regions, for example cooling over the Iceland Basin and more intensive mixing over the shallow IFR, lead to different water properties of the inflow branches (Rossby et al., 2018). Hence, a correct simulation of the different inflow branches is important also for reproducing the right northward transport of heat. This, in turn, is crucial for subsequent water mass transformations in the Nordic Seas and hence the for the overturning circulation.

Also an improved simulation of the overflow strength and depth can help in reproducing a realistic overturning circulation. With the nest, our model system features more and deeper overflow over the Iceland–Scotland Ridge, which constitutes about a third of the production of North Atlantic Deep Water (Devana and Johns, 2024). With the nest's ability to simulate a more confined and deep overflow bottom current, it hence contributes to a better representation of the lower limb of the AMOC (de Marez et al., 2024).

Therefore, it might be promising to adopt the presented nesting approach to large-scale climate models. Roberts et al. (2020) state that overflows from the Nordic Seas are still poorly represented in even the highest-resolution global models available, but in their study they show that higher resolution climate models in general simulate a stronger AMOC. To increase the resolution

https://doi.org/10.5194/egusphere-2026-5283
Preprint. Discussion started: 3 September 2026

of a global model in the whole domain however, would make the simulations computationally extremely expensive. A nest would require less additional computational resources. How much that would be, depends on many parameters like the size of the nested domain, the frequency of writing model output, etc. For our specific case, adding a nest of 293×194 grid cells into a parent domain of 781×888 grid cells and refining the resolution by a factor of 3 in both space and time, increased the computational time by about 70%. Even though our parent model has a quite different resolution than a typical climate model, our results seem to indicate that a nesting approach could improve the simulated exchanges over the ridge in a computationally efficient way – possibly also in climate models.

The Nested model setup can be used for further investigations, as it has proven to realistically simulate the exchange of water masses over the Iceland–Scotland Ridge without assimilation or restoring. For example, due to its ability to resolve eddying features, it could be used to study entrainment processes on the IFR. Its high resolution also enables investigations of the Iceland–Faroe Ridge overflow, specifically its locations and the possible interaction with the inflow (Hansen et al., 2018; Larsen et al., 2026). The tracer approach could be useful to explore the overflow pathways and along-path entrainment in more detail.

5 Conclusion

In this study, we show that using a two-way high-resolution nest in the area between Iceland and Scotland can improve the simulation of water transports around the Faroe Islands in various aspects:

- The inflow of Atlantic water towards the Nordic Seas is more realistic both in the Faroe–Shetland Channel and over the Iceland–Faroe Ridge (as observed at Section N).
- The overflow strength of dense water through the Faroe Bank Channel increases and agrees well with observations.
- The nest increases the daily variability of the water flows, which is in accordance with observations in the FBC.
- Dye passive tracers reveal that overflow waters stay more confined and sink deeper after crossing the Iceland–Scotland Ridge.

This indicates a potential to use localized, high-resolution nests in large scale models as a computationally efficient way to improve the simulation of water transports as key components of the large-scale ocean circulation.

Code and data availability.

- NEMO is an open-source community ocean model (https://nemo-ocean.eu/). This study is conducted with NEMO version 4.0.4, revision 13658.
- The ORCA12 bathymetry used in the nest has been downloaded from http://gws-access.ceda.ac.uk/public/nemo/runs/ORCA0083-N06/domain/bathymetry_ORCA12_V3.3.nc (last accessed on 2025-07-29).

https://doi.org/10.5194/egusphere-2026-5283
Preprint. Discussion started: 3 September 2026

450 – The ORAS5 data used to initialize the model in September 2007 (described in https://www.cen.uni-hamburg.de/en/icdc/data/ocean/easy-init-ocean/ecmwf-oras5.html) are downloaded from ICDC: http://icdc.cen.uni-hamburg.de/thredds/fileServer/ftpthredds/EASYInit/oras5/ORCA025/votemper/opa0/VARIABLE_ORAS5_1m_200709_grid_T_02.nc for VARIABLESs: votemper, vosaline, ileadfra and iicethic (last accessed on 2025-08-13).

– The GLORYS data used as boundary conditions can be downloaded through the Copernicus Marine Service: https://doi.org/10.48670/
455 moi-00021

– The altimeter product used for SSH evaluation and for the FSC observation time series can be downloaded through the Copernicus Marine Service: https://doi.org/10.48670/moi-00148

– The observations of water transport in the FBC and at Section N are available at: https://www.envofar.fo/index.php?page=climate (last accessed on 2026-08-27).

460 Appendix A: Settings and parameters of the model setups

A summary of relevant settings and parameters used for the model simulations is given in Table A1.

Appendix B: Sensitivity of the Faroe Bank Channel overflow calculation on model output frequency

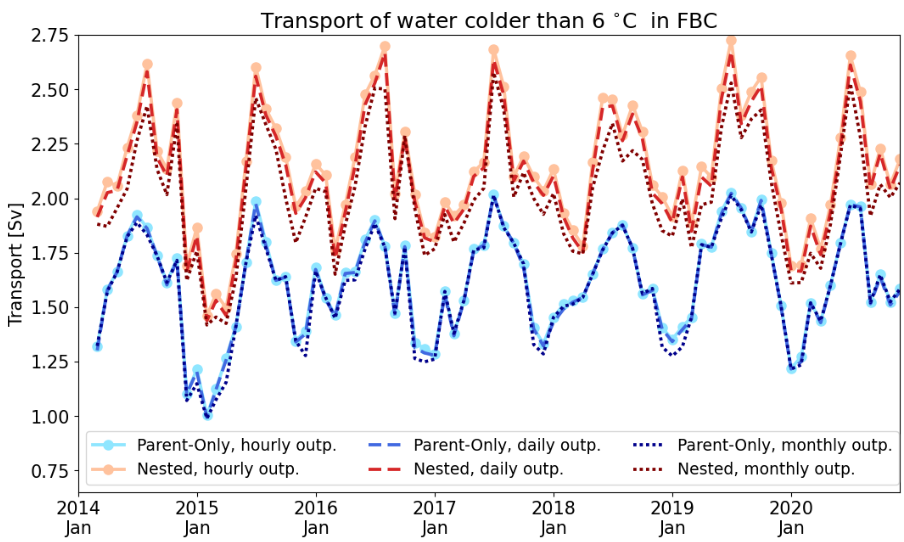

Figure B1. Monthly average transport of water colder than 6 °C in the Faroe Bank Channel for the Parent-Only simulation (blue) and the Nested simulation (red). The different line styles represent overflow transport calculated based on hourly model output (solid line, same as in Fig. 5), daily model output (dashed line), and monthly model output (dotted line), respectively.

For all calculations of water mass transports through sections in this study, we use hourly model output of water temperature/salinity and volume transport. If hourly output was not available and the water mass transport had to be calculated based

https://doi.org/10.5194/egusphere-2026-5283
Preprint. Discussion started: 3 September 2026

Table A1. NEMO model settings and parameters.

General settings:	
Vertical grid	75 vertical layers ($z^{\star}$-coordinate with partial steps and non-linear free surface)
Time step	Parent: 600 s, Nest: 200 s
Restoring of T or S	OFF
Surface boundary condition	Bulk formula
Inverse barometer effect	ON
Tides	Tidal potential and forcing from the boundaries
Tidal constituents	M2, K1, K2, N2, O1, P1, Q1, S2
Bottom boundary layer parametrization	diffusive BBL
Top/Bottom drag	Logarithmic drag. Coefficients: $2.5 \cdot 10^{-3}$ (top) and $5 \cdot 10^{-4}$ (bottom)
Temperature and salinity:	
Tracer advection scheme	FCT 4th order horizontal, 2nd order vertical
Lateral diffusion of tracer	Bilaplacian operator, iso-neutral with method of stabilizing correction
Eddy coefficient	Dependent on local velocity and grid-spacing
Mixed layer eddy parametrisation (Fox-Kemper)	OFF
Eddy induced velocity parametrization	OFF
Dynamics:	
Momentum advection	Parent: Vector form, 2nd order centered scheme
	Nest: 3rd order UBS (Upstream Biased Scheme)
Vorticiy/Coriolis scheme	Energy and enstrophy conserving scheme
Hydrostatic pressure gradient	s-coordinate (standard jacobian formulation)
Surface pressure gradient	Split-explicit free surface with time filtering of barotropic variables
Lateral diffusion of momentum	Parent: Laplacian operator, iso-level with mixing coefficients dependent on mesh size and depth with 0.1 m s^{-1} lateral viscous velocity
	Nest: OFF
Vertical physics:	
Adaptive-implicit vertical advection	ON
Vertical closure	Generic Length Scale scheme with k–ϵ closure
Enhanced vertical diffusion	applied on tracer with mixing coefficient 10 m^2/s
Double diffusion mixing	ON
Vertical eddy viscosity	10^{-5} m^2/s
Vertical eddy diffusivity	10^{-6} m^2/s

https://doi.org/10.5194/egusphere-2026-5283
Preprint. Discussion started: 3 September 2026

on daily or monthly model output, the results would become slightly inaccurate. Figure B1 illustrates this for the FBC section: If monthly output data is used (dotted line), the overflow transport is underestimated by 0.12 Sv in the Nested simulation and by 0.02 Sv in the Parent-Only simulation. The reason lies in the use of a masking for “water colder than 6 °C”. If water temperatures vary quickly, then a monthly average might include (or exclude) water flow with higher (or lower) temperatures. The calculation becomes more inaccurate the coarser the time resolution is compared to the variability of the water flow. Therefore, the Nested simulation suffers more from this effect because it exhibits a higher daily variability than the Parent-Only simulation. Using daily model output (dashed line in Fig. B1) reduces the underestimation of the overflow transport to 0.03 Sv for the Nested simulation and it removes it for the Parent-Only simulation.

Author contributions. All authors contributed to the conceptualization of the study and to writing (reviewing and editing). AMUG developed the nested model, conducted the model simulations, analysed and visualized the results and wrote the manuscript draft. SMO helped with designing the methodology and contributed to the investigations. BH created and provided some of the evaluation data. BH and KMHL provided some text for the original draft.

Competing interests. The authors declare that they have no conflict of interest.

Acknowledgements. This work is financially supported by the Danish Government as part of the National Centre for Climate Research (NCKF) and partly supported by the ObsSea4Clim project funded by the European Union, Grant Agreement number: 101136548, contribution Nr. 62. We thank Robinson Hordoir for providing the model setup for the parent domain (using version NEMO 3.6) and we thank Hjálmar Hátún for enlightning discussions during the preliminary scoping. This study has been conducted using E.U. Copernicus Marine Service Information: 10.48670/moi-00021 and 10.48670/moi-00148. Data have been processed using CDO (Schulzweida, 2023) and Python.

https://doi.org/10.5194/egusphere-2026-5283
Preprint. Discussion started: 3 September 2026

References

Adcroft, A., Anderson, W., Balaji, V., Blanton, C., Bushuk, M., Dufour, C. O., Dunne, J. P., Griffies, S. M., Hallberg, R., Harrison, M. J., Held, I. M., Jansen, M. F., John, J. G., Krasting, J. P., Langenhorst, A. R., Legg, S., Liang, Z., McHugh, C., Radhakrishnan, A., Reichl, B. G., Rosati, T., Samuels, B. L., Shao, A., Stouffer, R., Winton, M., Wittenberg, A. T., Xiang, B., Zadeh, N., and Zhang, R.: The GFDL Global Ocean and Sea Ice Model OM4.0: Model Description and Simulation Features, Journal of Advances in Modeling Earth Systems, 11, 3167–3211, https://doi.org/10.1029/2019ms001726, 2019.

Beaird, N. L., Rhines, P. B., and Eriksen, C. C.: Overflow Waters at the Iceland–Faroe Ridge Observed in Multiyear Seaglider Surveys, Journal of Physical Oceanography, 43, 2334–2351, https://doi.org/10.1175/JPO-D-13-029.1, 2013.

Beaird, N. L., Rhines, P. B., and Eriksen, C.: Observations of seasonal subduction at the Iceland-Faroe Front, Journal of Geophysical Research: Oceans, 121, 4026–4040, https://doi.org/10.1002/2015jc011501, 2016.

Berx, B., Hansen, B., Østerhus, S., Larsen, K. M., Sherwin, T., and Jochumsen, K.: Combining in situ measurements and altimetry to estimate volume, heat and salt transport variability through the Faroe–Shetland Channel, Ocean Science, 9, 639–654, https://doi.org/10.5194/os-9-639-2013, 2013.

Bezaud, M., Deshayes, J., Ethé, C., Gehlen, M., and Orr, J.: PISCES biogeochemistry in a global NEMO configuration with double AGRIF nesting, in: DRAKKAR Ocean Modelling Workshop, https://drakkar2026.sciencesconf.org/, 2026.

Biastoch, A., Sein, D., Durgadoo, J. V., Wang, Q., and Danilov, S.: Simulating the Agulhas system in global ocean models – nesting vs. multi-resolution unstructured meshes, Ocean Modelling, 121, 117–131, https://doi.org/10.1016/j.ocemod.2017.12.002, 2018.

Bringedal, C., Eldevik, T., Skagseth, Ø., Spall, M. A., and Østerhus, S.: Structure and Forcing of Observed Exchanges across the Greenland–Scotland Ridge, Journal of Climate, 31, 9881–9901, https://doi.org/10.1175/jcli-d-17-0889.1, 2018.

Bruciaferri, D., Guiavarc'h, C., Hewitt, H. T., Harle, J., Almansi, M., Mathiot, P., and Colombo, P.: Localized General Vertical Coordinates for Quasi-Eulerian Ocean Models: The Nordic Overflows Test-Case, Journal of Advances in Modeling Earth Systems, 16, https://doi.org/10.1029/2023ms003893, 2024.

Childers, K.: Circulation and Transport Across the Iceland Faroes Shetland Ridge, Ph.D. thesis, Stony Brook Theses and Dissertations Collection, 2006-2020 (closed to submissions), 3568, https://commons.library.stonybrook.edu/stony-brook-theses-and-dissertations-collection/3568/, 2014.

Colombo, P., Barnier, B., Penduff, T., Chanut, J., Deshayes, J., Molines, J.-M., Le Sommer, J., Verezemskaya, P., Gulev, S., and Treguier, A.-M.: Representation of the Denmark Strait overflow in a z-coordinate eddying configuration of the NEMO (v3.6) ocean model: resolution and parameter impacts, Geoscientific Model Development, 13, 3347–3371, https://doi.org/10.5194/gmd-13-3347-2020, 2020.

de Marez, C., Ruiz-Angulo, A., and Le Corre, M.: Structure of the Bottom Boundary Current South of Iceland and Spreading of Deep Waters by Submesoscale Processes, Geophysical Research Letters, 51, https://doi.org/10.1029/2023gl107508, 2024.

de Marez, C., Ruiz-Angulo, A., and Gula, J.: Mesoscale Induced Vertical Fluxes Over the Iceland-Faroe Ridge, Geophysical Research Letters, 52, https://doi.org/10.1029/2025gl115520, 2025.

Debreu, L., Vouland, C., and Blayo, E.: AGRIF: Adaptive grid refinement in Fortran, Computers & Geosciences, 34, 8–13, https://doi.org/10.1016/j.cageo.2007.01.009, 2008.

Devana, M. and Johns, W.: Structure and Variability of Iceland Scotland Overflow Water Transport in the Western Iceland Basin, Journal of Geophysical Research: Oceans, 129, https://doi.org/10.1029/2023jc020107, 2024.

Doblas-Reyes, F. J., Kontkanen, J., Sandu, I., Acosta, M., Al Turjmam, M. H., Alsina-Ferrer, I., Andrés-Martínez, M., Anerdi, C., Arriola, L., Axness, M., Batlle Martín, M., Bauer, P., Becker, T., Beltrán, D., Beyer, S., Bockelmann, H., Bretonnière, P.-A., Cabaniols, S., Caprioli, S., Castrillo, M., Chandrasekar, A., Cheedela, S., Correal, V., Danovaro, E., Davini, P., Enkovaara, J., Frauen, C., Früh, B., Gaya Àvila, A., Ghinassi, P., Ghosh, R., Ghosh, S., González, I., Grayson, K., Griffith, M., Hadade, I., Haine, C., Hartick, C., Haus, U.-U., Hearne, S., Järvinen, H., Jiménez, B., John, A., Juchem, M., Jung, T., Kegel, J., Kelbling, M., Keller, K., Kinoshita, B., Kiszler, T., Klocke, D., Kluft, L., Koldunov, N., Kölling, T., Kolstela, J., Kornblueh, L., Kosukhin, S., Lacima-Nadolnik, A., Leal Rojas, J. J., Lehtiranta, J., Lunttila, T., Luoma, A., Manninen, P., Medvedev, A., Milinski, S., Mohammed, A., Müller, S., Naryanappa, D., Nazarova, N., Niemelä, S., Niraula, B., Nortamo, H., Nummelin, A., Nurisso, M., Ortega, P., Paronuzzi, S., Pedruzo-Bagazgoitia, X., Pelletier, C., Peña, C., Polade, S., Pradhan, H. K., Quintanilla, R., Quintino, T., Rackow, T., Räisänen, J., Rajput, M. M., Redler, R., Reuter, B., Rocha Monteiro, N., Roura-Adserias, F., Ruppert, S., Sayed, S., Schnur, R., Sharma, T., Sidorenko, D., Sievi-Korte, O., Soret, A., Steger, C., Stevens, B., Streffing, J., Sunny, J., Tenorio, L., Thober, S., Tigerstedt, U., Tinto, O., Tonttila, J., Tuomenvirta, H., Tuppi, L., Van Thielen, G., Vitali, E., von Hardenberg, J., Wagner, I., Wedi, N., Wehner, J., Willner, S., Yepes-Arbós, X., Ziemen, F., and Zimmermann, J.: The Destination Earth digital twin for climate change adaptation, Geoscientific Model Development, 19, 2821–2848, https://doi.org/10.5194/gmd-19-2821-2026, 2026.

Eriksdóttir, G., Hansen, B., Larsen, K. M. H., Olsen, S. M., Gierisch, A. M. U., and Ólafsdóttir, S. R.: Water mass modification of the warm Atlantic Inflow towards the Arctic across the Iceland-Faroe Ridge, Ocean Science, 22, 2405–2423, https://doi.org/10.5194/os-22-2405-2026, 2026.

Guo, C., Ilicak, M., Fer, I., Darelius, E., and Bentsen, M.: Baroclinic Instability of the Faroe Bank Channel Overflow*, Journal of Physical Oceanography, 44, 2698–2717, https://doi.org/10.1175/jpo-d-14-0080.1, 2014.

Hansen, B., Hátún, H., Kristiansen, R., Olsen, S. M., and Østerhus, S.: Stability and forcing of the Iceland-Faroe inflow of water, heat, and salt to the Arctic, Ocean Science, 6, 1013–1026, https://doi.org/10.5194/os-6-1013-2010, 2010.

Hansen, B., Larsen, K. M. H., Hátún, H., Kristiansen, R., Mortensen, E., and Østerhus, S.: Transport of volume, heat, and salt towards the Arctic in the Faroe Current 1993–2013, Ocean Science, 11, 743–757, https://doi.org/10.5194/os-11-743-2015, 2015.

Hansen, B., Larsen, K. M. H., Olsen, S. M., Quadfasel, D., Jochumsen, K., and Østerhus, S.: Overflow of cold water across the Iceland–Faroe Ridge through the Western Valley, Ocean Science, 14, 871–885, https://doi.org/10.5194/os-14-871-2018, 2018.

Hansen, B., Larsen, K. M. H., Hátún, H., Olsen, S. M., Gierisch, A. M. U., Østerhus, S., and Ólafsdóttir, S. R.: The Iceland–Faroe warm-water flow towards the Arctic estimated from satellite altimetry and in situ observations, Ocean Science, 19, 1225–1252, https://doi.org/10.5194/os-19-1225-2023, 2023.

Hansen, B. and Østerhus, S.: North Atlantic–Nordic Seas exchanges, Progress in Oceanography, 45, 109–208, https://doi.org/10.1016/s0079-6611(99)00052-x, 2000.

Hansen, B. and Østerhus, S.: Faroe Bank Channel overflow 1995–2005, Progress in Oceanography, 75, 817–856, https://doi.org/10.1016/j.pocean.2007.09.004, 2007.

Hersbach, H., Bell, B., Berrisford, P., Hirahara, S., Horányi, A., Muñoz-Sabater, J., Nicolas, J., Peubey, C., Radu, R., Schepers, D., Simmons, A., Soci, C., Abdalla, S., Abellan, X., Balsamo, G., Bechtold, P., Biavati, G., Bidlot, J., Bonavita, M., De Chiara, G., Dahlgren, P., Dee, D., Diamantakis, M., Dragani, R., Flemming, J., Forbes, R., Fuentes, M., Geer, A., Haimberger, L., Healy, S., Hogan, R. J., Hólm, E., Janisková, M., Keeley, S., Laloyaux, P., Lopez, P., Lupu, C., Radnoti, G., de Rosnay, P., Rozum, I., Vamborg, F., Villaume, S., and Thépaut, J.: The ERA5 global reanalysis, Quarterly Journal of the Royal Meteorological Society, 146, 1999–2049, https://doi.org/10.1002/qj.3803, 2020.

Hewitt, H. T., Bell, M. J., Chassignet, E. P., Czaja, A., Ferreira, D., Griffies, S. M., Hyder, P., McClean, J. L., New, A. L., and Roberts, M. J.: Will high-resolution global ocean models benefit coupled predictions on short-range to climate timescales?, Ocean Modelling, 120, 120–136, https://doi.org/10.1016/j.ocemod.2017.11.002, 2017.

Hewitt, H. T., Roberts, M., Mathiot, P., Biastoch, A., Blockley, E., Chassignet, E. P., Fox-Kemper, B., Hyder, P., Marshall, D. P., Popova, E., Treguier, A.-M., Zanna, L., Yool, A., Yu, Y., Beadling, R., Bell, M., Kuhlbrodt, T., Arsouze, T., Bellucci, A., Castruccio, F., Gan, B., Putrasahan, D., Roberts, C. D., Van Roekel, L., and Zhang, Q.: Resolving and Parameterising the Ocean Mesoscale in Earth System Models, Current Climate Change Reports, 6, 137–152, https://doi.org/10.1007/s40641-020-00164-w, 2020.

Hordoir, R., Skagseth, Ø., Ingvaldsen, R. B., Sandø, A. B., Löptien, U., Dietze, H., Gierisch, A. M. U., Assmann, K. M., Lundesgaard, Ø., and Lind, S.: Changes in Arctic Stratification and Mixed Layer Depth Cycle: A Modeling Analysis, Journal of Geophysical Research: Oceans, 127, https://doi.org/10.1029/2021jc017270, 2022.

Hordoir, R., Berntsen, J., Hieronymus, M., Pemberton, P., and Hátún, H.: Revisiting the parameterization of dense water plume dynamics in geopotential coordinates in NEMO v4.2.2, Geoscientific Model Development, 19, 2677–2690, https://doi.org/10.5194/gmd-19-2677-2026, 2026.

Jackson, L. C., Hewitt, H. T., Bruciaferri, D., Calvert, D., Graham, T., Guiavarc'h, C., Menary, M. B., New, A. L., Roberts, M., and Storkey, D.: Challenges simulating the AMOC in climate models, Philosophical Transactions of the Royal Society A: Mathematical, Physical and Engineering Sciences, 381, https://doi.org/10.1098/rsta.2022.0187, 2023.

Larsen, K. M. H., Hansen, B., Hátún, H., Johansen, G. E., Østerhus, S., and Olsen, S. M.: The Coldest and Densest Overflow Branch Into the North Atlantic is Stable in Transport, But Warming, Geophysical Research Letters, 51, https://doi.org/10.1029/2024gl110097, 2024.

Larsen, K. M. H., Eriksdóttir, G., Hansen, B., Hátún, H., Olsen, S. M., and Østerhus, S.: Iceland-Faroe overflow revealed by in-situ observations, Nature Communications, https://doi.org/10.1038/s41467-026-77220-w, 2026.

Madec, G., Bourdallé-Badie, R., Chanut, J., Clementi, E., Coward, A., Ethé, C., Iovino, D., Lea, D., Lévy, C., Lovato, T., Martin, N., Masson, S., Mocavero, S., Rousset, C., Storkey, D., Vancoppenolle, M., Müeller, S., Nurser, G., Bell, M., and Samson, G.: NEMO Ocean Engine Version 4.0.1, Zenodo, https://doi.org/10.5281/ZENODO.3878122, 2019.

NEMO TOP Working Group: TOP – Tracers in Ocean Paradigm – The NEMO Tracers engine, Scientific Notes of Climate Modelling Center, 28, ISSN 1288-1619, Institut Pierre-Simon Laplace (IPSL), https://doi.org/10.5281/ZENODO.1471700, 2018.

Olsen, S. M., Hansen, B., Quadfasel, D., and Østerhus, S.: Observed and modelled stability of overflow across the Greenland–Scotland ridge, Nature, 455, 519–522, https://doi.org/10.1038/nature07302, 2008.

Riemenschneider, U. and Legg, S.: Regional simulations of the Faroe Bank Channel overflow in a level model, Ocean Modelling, 17, 93–122, https://doi.org/10.1016/j.ocemod.2007.01.003, 2007.

Roberts, M. J., Jackson, L. C., Roberts, C. D., Meccia, V., Docquier, D., Koenigk, T., Ortega, P., Moreno-Chamarro, E., Bellucci, A., Coward, A., Drijfhout, S., Exarchou, E., Gutjahr, O., Hewitt, H., Iovino, D., Lohmann, K., Putrasahan, D., Schiemann, R., Seddon, J., Terray, L., Xu, X., Zhang, Q., Chang, P., Yeager, S. G., Castruccio, F. S., Zhang, S., and Wu, L.: Sensitivity of the Atlantic Meridional Overturning Circulation to Model Resolution in CMIP6 HighResMIP Simulations and Implications for Future Changes, Journal of Advances in Modeling Earth Systems, 12, https://doi.org/10.1029/2019ms002014, 2020.

Rossby, T., Prater, M. D., and Søiland, H.: Pathways of inflow and dispersion of warm waters in the Nordic seas, Journal of Geophysical Research: Oceans, 114, https://doi.org/10.1029/2008jc005073, 2009.

https://doi.org/10.5194/egusphere-2026-5283
Preprint. Discussion started: 3 September 2026

Rossby, T., Flagg, C., Chafik, L., Harden, B., and Søiland, H.: A Direct Estimate of Volume, Heat, and Freshwater Exchange Across the Greenland-Iceland-Faroe-Scotland Ridge, Journal of Geophysical Research: Oceans, 123, 7139–7153, https://doi.org/10.1029/2018jc014250, 2018.

Saunders, P. M.: The Flux of Dense Cold Overflow Water Southeast of Iceland, Journal of Physical Oceanography, 26, 85–95, https://doi.org/10.1175/1520-0485(1996)026<0085:tfodco>2.0.co;2, 1996.

Saunders, P. M.: Chapter 5.6 The dense northern overflows, in: Ocean Circulation and Climate, edited by Siedler, G., Church, J., and Gould, J., vol. 77 of *International Geophysics*, pp. 401–417, Academic Press, https://doi.org/https://doi.org/10.1016/S0074-6142(01)80131-5, 2001.

Schulzweida, U.: CDO User Guide, https://doi.org/10.5281/zenodo.10020800, 2023.

Talandier, C., Deshayes, J., Treguier, A.-M., Capet, X., Benshila, R., Debreu, L., Dussin, R., Molines, J.-M., and Madec, G.: Improvements of simulated Western North Atlantic current system and impacts on the AMOC, Ocean Modelling, 76, 1–19, https://doi.org/10.1016/j.ocemod.2013.12.007, 2014.

Wang, H., Legg, S. A., and Hallberg, R. W.: Representations of the Nordic Seas overflows and their large scale climate impact in coupled models, Ocean Modelling, 86, 76–92, https://doi.org/10.1016/j.ocemod.2014.12.005, 2015.

Xu, X., Schmitz, W. J., Hurlburt, H. E., Hogan, P. J., and Chassignet, E. P.: Transport of Nordic Seas overflow water into and within the Irminger Sea: An eddy-resolving simulation and observations, Journal of Geophysical Research: Oceans, 115, https://doi.org/10.1029/2010jc006351, 2010.

Zhang, R., Delworth, T. L., Rosati, A., Anderson, W. G., Dixon, K. W., Lee, H.-C., and Zeng, F.: Sensitivity of the North Atlantic Ocean Circulation to an abrupt change in the Nordic Sea overflow in a high resolution global coupled climate model, Journal of Geophysical Research, 116, https://doi.org/10.1029/2011jc007240, 2011.

Zuo, H., Balmaseda, M. A., Tietsche, S., Mogensen, K., and Mayer, M.: The ECMWF operational ensemble reanalysis–analysis system for ocean and sea ice: a description of the system and assessment, Ocean Science, 15, 779–808, https://doi.org/10.5194/os-15-779-2019, 2019.

Østerhus, S., Woodgate, R., Valdimarsson, H., Turrell, B., de Steur, L., Quadfasel, D., Olsen, S. M., Moritz, M., Lee, C. M., Larsen, K. M. H., Jónsson, S., Johnson, C., Jochumsen, K., Hansen, B., Curry, B., Cunningham, S., and Berx, B.: Arctic Mediterranean exchanges: a consistent volume budget and trends in transports from two decades of observations, Ocean Science, 15, 379–399, https://doi.org/10.5194/os-15-379-2019, 2019.